

Plastic strain localization

Mfano Africa-Oxford Research Report

Joel-Pascal Ntwali N’konzi (supervised by Richard Katz)

June–August 2021

1 Introduction

Strain localisation is a phenomenon that occurs in materials when plastic strain increments are localised into narrow zones of increased deformation [SG19]. Its most common manifestations are *shear band* formation and *necking*. Strain localisation has been related to failure in materials, making its analysis of great relevance.

The phenomenon can be characterized as a loss of stability of a homogeneously deformed steady state of the material [SG19]. For example, necking occurs as an material instability during tensile tests. Prior to necking, plastic deformations are evenly distributed through the entire material. But as the applied tensile force is being increased, the plastic strain increments stop being evenly distributed as they get kind of ‘trapped’ in a relatively smaller region in the material, forming a *neck of deformation* (see Figure 1). Though plastic deformations get localized in the neck, elastic deformations might still occur in the remaining part of the material after the onset of necking [Wik].

One of challenges in the numerical simulations is that strain localization generally induces a loss of ellipticity of the steady-state governing equations in the classical description of materials (Cauchy continuum), which results in mesh-size dependency in Fine Elements simulations [SG19]. To circumvent this issue, different *regularization* techniques have been investigated in the literature. In this report, we will explore viscous regularization and Cosserat continuum.

In this report, we give an introduction to the analysis of strain localization using stability analysis. The rest of the report is organized as follows. In Section 2, we review the basic concepts on the mathematical description of materials and different deformation modes. In Section 3, we introduce the perturbation theory approach for strain localization and use it to derive the localization condition for a one-dimensional elastoplastic material under simple shearing. We conclude the section by showing the failure of viscous regularization. In Section 4, we explore the Cosserat continuum theory and how it can be used to regularize the strain localization problem.

2 Governing equations and constitutive laws

When a force is applied to a material, it deforms. From everyday experience, it is natural to assume that the extent of the deformation, depends on of applied *stress*, but also on the specific material. This intuition is formalized by the concept of *constitutive law*, which relate the applied stress to the resulting *strain*, or deformation [How17]. In addition, as the material deforms, some quantities such as the momentum and kinetic energy will be conserved. These conservation laws allow to derive the *governing equations* of the system under study. These equations describe how the material under straining will evolve in time and space.

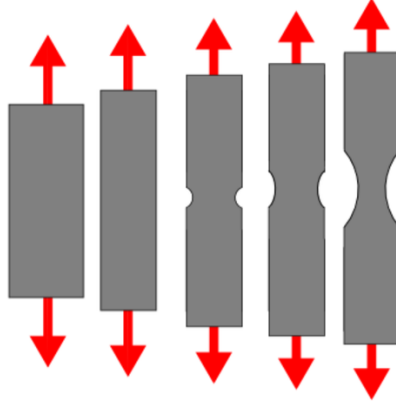


Figure 1: Schematic diagram of necking. Prior to necking, plastic strains are evenly distributed in the material. After the onset of necking, plastic deformations (compression) will occur only in the necked part of the material under load (credit: Wikipedia).

In the classical approach, materials are described as continuous distribution of particles, each being represented by a point and characterized kinematically by a velocity u_i . In that case, the Cauchy momentum equation describes the evolution of the system under deformation, and is given by:

$$\rho \frac{\partial^2 u_i}{\partial t^2} = \rho g_i + \frac{\partial \sigma_{ij}}{\partial x_j}; \quad (2.1)$$

where ρg_i is the body force vector, σ_{ij} is the stress tensor, and Einstein summation convention has been used [How17]. Moreover, the strain tensor is defined by

$$\varepsilon_{ij} = \frac{1}{2} \left(\frac{\partial u_i}{\partial x_j} + \frac{\partial u_j}{\partial x_i} \right). \quad (2.2)$$

The very common experience of stretching rubber bands suggests that in some cases the material will return to its initial shape and size almost instantaneously once the load is removed, in which case the deformation is called *elastic*. In other cases, the material will undergo some irreversible deformations once the applied stress reaches some critical value, called *yield stress*. Such deformations will be referred to as *plastic* deformations. A common example of such a deformation comes from the experience of bending a paper clip. If it is bent a little, it snaps back to its original shape. But if it is bent a lot, it undergoes a permanent, plastic deformation.

Lastly, a solid material under deformation might behave partly like a fluid, showing some *viscous* effects. In that case, the applied stress is proportional to the *rate of deformation* when the material behaves like a Newtonian fluid. This kind of deformation is called *viscous* deformation and it generally occurs in combination with elastic and/or plastic deformations [Kel][How17].

Different constitutive relations describe these kinds of deformations as described below.

2.1 Elastic deformation

For small deformations ($\epsilon \ll 1$), nonlinear effects are negligible, and elastic deformations are described by the following constitutive law

$$\sigma_{ij} = K \varepsilon_{kk} \delta_{ij} + 2G \left(\varepsilon_{ij} - \frac{1}{3} \varepsilon_{kk} \delta_{ij} \right), \quad (2.3)$$

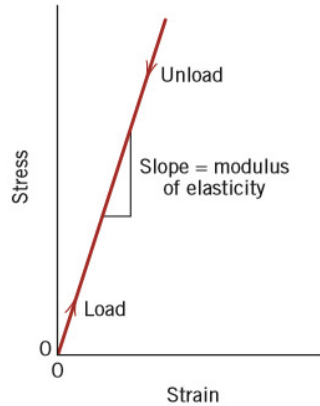


Figure 2: Stress-strain response for elastic deformation. The modulus of elasticity is called *Young's modulus*.

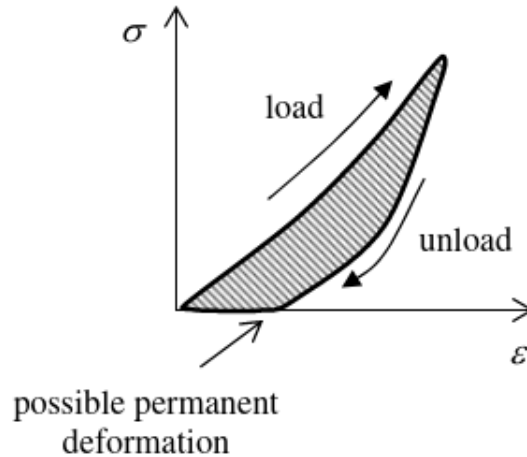


Figure 3: Stress-strain response for viscoelastic deformations. The loading and unloading curves do not coincide as there is a possibility of permanent deformations (credit: [Kel])

where K and G are material parameters describing its resistance to deformation, and are called *bulk modulus* and *shear modulus*, respectively. In this case, the stress-strain response is linear (see Figure 2), and the deformation is completely reversible upon unloading [Kel].

2.2 Viscoelastic deformation

As mentioned earlier, viscoelastic deformations are dependent on the *rate of straining* $\frac{d\varepsilon}{dt}$; i.e., the faster the stretching, the larger the stress required. In addition, with contrast to the elastic case, a viscoelastic straining might leave some permanent deformation upon complete unloading. As a result, the loading and unloading curves do not coincide (see Figure 3) [Kel].

The simplest descriptions of viscoelastic deformations are the *Maxwell* and *Kelvin* models. The Maxwell model describes the material as a combination of a linear spring and dash-pot in series. In that case, they share the same stress σ and the total strain $\varepsilon = \varepsilon^e + \varepsilon^v$ is the sum of the elastic strain ε^e of the spring and the viscous strain ε^v of the dash-pot. The constitutive relations of the two

sub-systems are respectively given by:

$$\sigma = E\varepsilon^e \quad \text{and} \quad \sigma = \eta\dot{\varepsilon}^v; \quad (2.4)$$

where we focus on the scalar problem for simplicity.

Taking (2.4) into $\dot{\varepsilon} = \dot{\varepsilon}^e + \dot{\varepsilon}^v$ then yields:

$$\begin{aligned} \dot{\varepsilon} &= \dot{\varepsilon}^e + \dot{\varepsilon}^v \\ &= \frac{1}{E}\dot{\sigma} + \frac{1}{\eta}\sigma, \end{aligned}$$

from which we obtain the constitutive law:

$$\sigma + \frac{\eta}{E}\dot{\sigma} = \eta\dot{\varepsilon}, \quad (2.5)$$

where η is the viscosity of the fluid in the dash-pot and E is the *Young's modulus*. The two parameters describe the resistance of the material to deformation [Kel].

In the Kelvin description, the material is modeled as a linear spring and dash-pot in parallel. Hence, they are subjected to different stresses but undergo the same strain ε . If we let σ_e and σ_v be the stresses in the linear spring and the dash-pot, respectively, then total stress $\sigma = \sigma_e + \sigma_v$, and we have the following equations:

$$\sigma_e = E\varepsilon \quad \text{and} \quad \sigma_v = \eta\dot{\varepsilon}. \quad (2.6)$$

Taking these into $\dot{\sigma} = \dot{\sigma}_e + \dot{\sigma}_v$ then results into the following constitutive law:

$$\sigma = E\varepsilon + \eta\dot{\varepsilon}. \quad (2.7)$$

More complex rheological models are obtained by combining the Maxwell and Kelvin models in different ways (see [Kel]).

2.3 Elastoplastic deformations

Plastic deformations occur once the applied stress reaches a critical value called *yield stress*, and are rate-independent. Rate-dependent permanent deformations that occur once the yield stress is reached are classified as *viscoplastic* deformations [Kel]. In the plastic region, both elastic and plastic strains occur, and hence strain increments can be written as

$$d\varepsilon_{ij} = d\varepsilon_{ij}^e + d\varepsilon_{ij}^p, \quad (2.8)$$

where $d\varepsilon^e$ and $d\varepsilon^p$ are the elastic and plastic strain increments, respectively [SG19]. Plastic strain increments are related to the stress increments by

$$d\sigma_{ij} = H d\varepsilon_{ij}^p, \quad (2.9)$$

where H is called *plastic modulus* [Kel]. Moreover, constitutive laws are in general given by the following equation:

$$d\varepsilon_{ij}^p = d\lambda \frac{dg}{d\sigma_{ij}}, \quad (2.10)$$

where the *plastic multiplier* λ depends on the specific yield criterion and g is the called *plastic potential*. When g is equal to the yield function f , (2.10) is called *associated flow-rule*. Otherwise, it is called *non-associated flow rule*. It is noteworthy that almost all the realistic problems in plasticity are modeled by a non-associated flow rule [Kel].

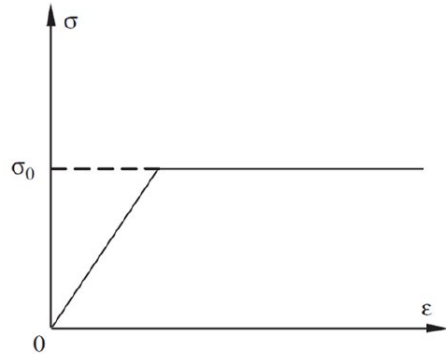


Figure 4: Stress-strain response for an elastic-perfectly plastic material. Once the yield stress σ_0 is reached, there is no need for additional stress for the material to continue to deform.

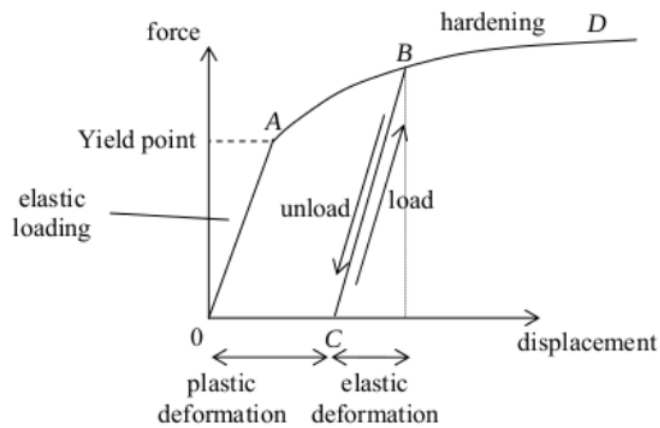


Figure 5: Stress-strain response for a plastic strain hardening material. In the plastic region, more stress is needed to achieve additional deformation (credit: [Kel]).

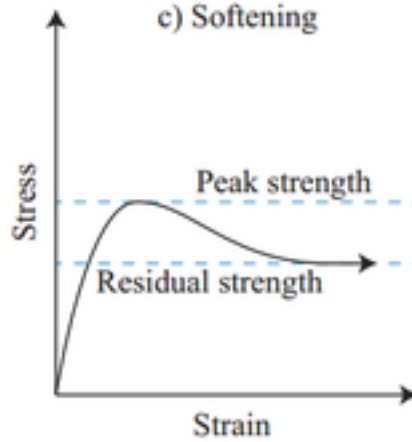


Figure 6: Stress-strain response for a strain softening material in the plastic region (credit:L. Teymour).

Lastly, it is important to note that there are three modes of plastic deformations, which are determined by the *hardening modulus* $h = \frac{H}{2G} > -1$. When $h = 0$, the material is said to be *perfectly plastic* (see Figure 4). If $h > 0$, the material undergoes *strain hardening*, and additional stress is needed to further deform the material (see Figure 5).

The last type of plastic response corresponds to the case where less stress is needed to achieve additional strains once the material yields (see Figure 6). In that case, $h < 0$ and the material is said to undergo *strain softening* [Kel].

3 Instances and solutions

As stated earlier, the onset of strain localization mathematically characterized as a loss of stability of a homogeneous deformation state. In this section, we show how perturbation theory can be used to derive the conditions under which strain localization can occur in Cauchy materials under elastoplastic and elasto-viscoplastic flow rules.

3.1 General approach

The stability analysis of a homogeneous deformation state for strain localization follows the following steps:

1. state the governing equations and constitutive laws describing the material under deformation;
2. assume a homogeneously deformed steady state $u_i = u_i^*$, $\sigma_{ij} = \sigma_{ij}^*$ and $\varepsilon_{ij} = \varepsilon_{ij}^*$;
3. perturb the kinematic field around the steady state, $u_i = u_i^* + \tilde{u}_i$;
4. find the governing equation and constitutive law describing the deformation;
5. assume the deformation is a plane wave $\tilde{u}_i = U_i e^{st+ikn_j x_j}$ and take this general form into the equations obtained in the previous step;
6. the preceding step yields an algebraic equation in s . If all the solutions of this equation are such that $\Re[s] \leq 0$, the perturbation will not grow and the homogeneous deformation is stable. Otherwise, the homogeneous deformation is unstable and any small perturbation from it will grow up, leading to an inhomogeneous deformation, which is the onset of strain localization.

In what follows, we apply this approach to an elastoplastic problem and a elasto-viscoplastic problem, and show that strain localization is expected under strain softening conditions. The two problems are taken from [SG19], and describe an infinite layer of material under simple shear. The system is assumed to be invariant in the x_1 and x_3 directions, so that the problems are one dimensional. We assume in addition that the flow is incompressible.

3.2 Elastoplastic problem

Here, the material is assumed to have an elastoplastic response, and the yield function is given by:

$$F = \sigma_{12} - \tau_0. \quad (3.1)$$

In the plastic region, strain increments are split in elastic and plastic parts as in (2.8); where elastic and plastic strain increments are described by (2.3) and (2.9), respectively.

As the system is invariant in the x_1 and x_3 directions, and we assumed incompressibility, the Cauchy's momentum equation (2.1) becomes:

$$\rho \ddot{u}_1 = \rho g_1 + \frac{\partial \sigma_{12}}{\partial x_2}. \quad (3.2)$$

We consider a homogeneous deformation at steady state ($\dot{u}_i = 0$) in the plastic region, i.e., $\sigma_{12} = \sigma_{12}^* = \tau_0$ and $u_1 = u_1^*$. This state will be stable as long as any perturbation does not grow in time. We perturb the displacement field as described in step 3. Then (3.2) yields

$$\rho \ddot{\tilde{u}}_1 = \frac{\partial \tilde{\sigma}_{12}}{\partial x_2}. \quad (3.3)$$

and from (2.3), we have

$$\begin{aligned} \tilde{\sigma}_{12} &= 2G \tilde{\varepsilon}_{12}^e \\ d\tilde{\sigma}_{12} &= 2G d\tilde{\varepsilon}_{12}^e \\ &= 2G(d\tilde{\varepsilon}_{12} - d\tilde{\varepsilon}_{12}^p) \quad \text{by (2.8)} \\ &= 2G \left(d\tilde{\varepsilon}_{12} - \frac{1}{H} d\tilde{\sigma}_{12} \right) \quad \text{by (2.9)} \\ \left(1 + \frac{2G}{H} \right) d\tilde{\sigma}_{12} &= 2G d\tilde{\varepsilon}_{12} \\ d\tilde{\sigma}_{12} &= \frac{2G}{1 + \frac{2G}{H}} d\tilde{\varepsilon}_{12} \\ &= 2G \frac{H}{2G \left(1 + \frac{H}{2G} \right)} d\tilde{\varepsilon}_{12}. \end{aligned}$$

Hence,

$$\tilde{\sigma}_{12} = 2G \left(\frac{h}{1+h} \right) \tilde{\varepsilon}_{12}. \quad (3.4)$$

As stated in Step 5, equation (3.3) admits a plane wave solution of the form

$$\tilde{u}_1 = U_1 e^{st+ikx_2}; \quad (3.5)$$

where the amplitude U_1 , the growth coefficient $s \in \mathbf{C}$, and the wavenumber k are constants. Taking this into (3.3) and (3.4) as described in Step 5, we obtain

$$\begin{aligned}
\rho s^2 \tilde{u}_1 &= \frac{\partial \tilde{\sigma}_{12}}{\partial x_2} \\
&= 2G \left(\frac{h}{1+h} \right) \frac{\partial \tilde{\epsilon}_{12}}{\partial x_2} \quad \text{by (3.4)} \\
&= 2G \left(\frac{h}{1+h} \right) \frac{\partial}{\partial x_2} \left[\frac{1}{2} \left(\frac{\partial \tilde{u}_1}{\partial x_2} + \underbrace{\frac{\partial \tilde{u}_2}{\partial x_1}}_0 \right) \right] \quad \text{by (2.2)} \\
&= G \left(\frac{h}{1+h} \right) \frac{\partial^2 \tilde{u}_1}{\partial x_2^2} \\
&= G \left(\frac{h}{1+h} \right) (ik)^2 \tilde{u}_1.
\end{aligned}$$

Hence,

$$\rho s^2 = G \left(\frac{h}{1+h} \right) (ik)^2,$$

and

$$s = \pm i k v_s \sqrt{\frac{h}{1+h}}; \quad (3.6)$$

where $v_s = \sqrt{\frac{G}{\rho}}$ is the S-wave phase speed.

As described in Step 6, the homogeneous deformation is unstable if $\mathcal{R}[s] > 0$. Equation (3.6) shows that this is equivalent to having $h < 0$. Therefore, *strain localization is expected when the material is strain softening*. In addition, the growth coefficient s is inversely proportional to the wavelength $\lambda = \frac{2\pi}{k}$, becoming infinite as $\lambda \rightarrow 0$ (see Figure 7). As a result, narrow perturbations will grow faster and the deformation band width is unrealistically zero, inducing mesh-size dependency in Finite Elements calculations [SG19]. To go around this issue, different regularization techniques have been proposed in the literature, with the goal of avoiding strain localization for zero wavelength. In the rest of this section, we examine viscous regularization and Cosserat regularization is investigated in the next section.

3.3 Elasto-viscoplastic problem

As shown below, introducing viscous effects slows down perturbations occurring at very small wavelengths. This alleviates mesh-size dependency but does not regularize the problem.

With contrast to the elasto-plastic problem, the material of the layer is assumed here to have an elasto-viscoplastic response. Hence, strain increments after yield are given by:

$$\dot{\epsilon}_{ij} = \dot{\epsilon}_{ij}^e + \dot{\epsilon}_{ij}^{vp}, \quad (3.7)$$

and the viscoplastic strain increments are assumed to be described by the Perzyna's model:

$$\dot{\epsilon}_{ij}^{vp} = \dot{\lambda} \frac{\partial F}{\partial \sigma_{ij}} \quad (3.8)$$

$$\text{and } \dot{\lambda} = \frac{F}{\eta f_0} \quad (3.9)$$

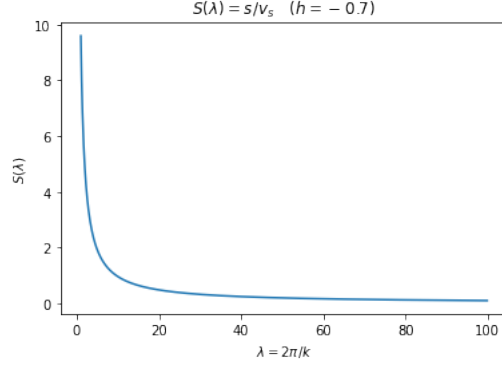


Figure 7: Growth coefficient vs wavelength of perturbation. Observe that small perturbations will grow faster. In addition, the fact that $s \rightarrow \infty$ as $\lambda \rightarrow 0$ has been associated to mesh-size dependency in FE calculations (see [SG19] for more details).

where η expresses viscosity, f_0 is the value of τ_0 at first yield, and the plastic modulus H is given by

$$\frac{d\tau_0}{d\varepsilon_{ij}^{vp}} = H. \quad (3.10)$$

The first step is to rewrite the constitutive law in a suitable form. From (3.1), we have:

$$\dot{F} = \dot{\sigma}_{12} - \frac{\partial \tau_0}{\partial \varepsilon_{12}^{vp}} \dot{\varepsilon}_{12}^{vp} \quad (3.11)$$

$$= \dot{\sigma}_{12} - H \dot{\varepsilon}_{12}^{vp}. \quad (3.12)$$

Taking (3.12) into (3.9) yields:

$$\dot{F} = \eta f_0 \ddot{\lambda} = \dot{\sigma}_{12} - H \dot{\varepsilon}_{12}^{vp}. \quad (3.13)$$

Plugging (3.7) into yields:

$$\begin{aligned} \dot{\sigma}_{12} &= H (\dot{\varepsilon}_{12} - \dot{\varepsilon}_{12}^e) + \eta f_0 \ddot{\lambda} \\ &= H \left(\dot{\varepsilon}_{12} - \frac{\dot{\sigma}_{12}}{2G} \right) + \eta f_0 \ddot{\lambda} \quad \text{by (2.3);} \end{aligned}$$

and

$$\left(1 + \frac{H}{2G} \right) \dot{\sigma}_{12} = H \dot{\varepsilon}_{12} + \eta f_0 \ddot{\lambda}.$$

As one has $\ddot{\lambda} = \ddot{\varepsilon}_{12}^{vp}$ by (3.1) & (3.8), the constitutive law can be written as:

$$\dot{\sigma}_{12} = 2G \frac{h}{1+h} \dot{\varepsilon}_{12} + \frac{\eta f_0}{1+h} \ddot{\varepsilon}_{12}^{vp}, \quad (3.14)$$

where $h = \frac{H}{2G}$ is the hardening modulus as before.

We now assume that the system is in a steady state of homogeneous deformation as in the previous problem. Assuming a perturbation $\tilde{u}_1 = u_1 - u_1^*$ from the homogeneous deformation of the form

$$\tilde{u}_1 = U_1 e^{st+ikx_2}, \quad (3.15)$$

we have:

$$\begin{aligned}
\ddot{\tilde{\epsilon}}_{12} &= \frac{1}{2} \frac{\partial \ddot{u}_{12}}{\partial x_2} & \dot{\tilde{\epsilon}}_{12}^e + \dot{\tilde{\epsilon}}_{12}^{vp} &= \dot{\tilde{\epsilon}}_{12} & \text{and } \dot{\tilde{\sigma}}_{12} &= 2G\dot{\tilde{\epsilon}}_{12}^e \\
&= s \frac{1}{2} \frac{\partial \dot{u}_{12}}{\partial x_2} & &= s\tilde{\epsilon}_{12} & &= 2Gs\tilde{\epsilon}_{12} \\
&= s\dot{\tilde{\epsilon}}_{12}; & &= s\tilde{\epsilon}_{12}^e + s\tilde{\epsilon}_{12}^{vp} & &= s\tilde{\sigma}_{12}. \\
& & \Rightarrow \dot{\tilde{\epsilon}}_{12}^e &= s\tilde{\epsilon}_{12}^e \text{ and } \dot{\tilde{\epsilon}}_{12}^{vp} &= s\tilde{\epsilon}_{12}^{vp}; & &
\end{aligned} \tag{3.16}$$

Taking (3.16) into (3.14) yields:

$$\tilde{\sigma}_{12} = 2G \frac{h}{1+h} \tilde{\epsilon}_{12} + \frac{\eta f_0}{1+h} \dot{\tilde{\epsilon}}_{12}^{vp}, \tag{3.17}$$

which, by (2.3) & (3.7), can be rewritten as:

$$\tilde{\sigma}_{12} = 2G \frac{h}{1+h} \tilde{\epsilon}_{12} + \frac{\eta f_0}{1+h} \dot{\tilde{\epsilon}}_{12} - \frac{1}{2G} \frac{\eta f_0}{1+h} \dot{\tilde{\sigma}}_{12}. \tag{3.18}$$

Now, (3.14) can be used in (3.18) in form of successive substitutions to give:

$$\tilde{\sigma}_{12} = 2G \frac{h}{1+h} \tilde{\epsilon}_{12} + \frac{\eta f_0}{(1+h)^2} \dot{\tilde{\epsilon}}_{12} - \frac{1}{2G} \frac{(\eta f_0)^2}{(1+h)^3} \ddot{\tilde{\epsilon}}_{12} + \frac{1}{4G^2} \frac{(\eta f_0)^3}{(1+h)^4} \ddot{\tilde{\sigma}}_{12} - \dots \tag{3.19}$$

Retaining only the first two terms of this series for simplicity, the constitutive law (3.19) for the perturbed system reads:

$$\tilde{\sigma}_{12} = 2G \frac{h}{1+h} \tilde{\epsilon}_{12} + \frac{\eta f_0}{(1+h)^2} \dot{\tilde{\epsilon}}_{12}. \tag{3.20}$$

From here, the idea is to proceed in the same way as we did for the elasto-plastic problem. In that regard, we take the general form (3.15) of the perturbation into the governing equation (3.3) and make use of the constitutive law (3.20) to obtain, after some algebra:

$$s^2 + v_s^2 \frac{\eta f_0}{2G(1+h)^2} k^2 s + v_s^2 \frac{h}{1+h} k^2 = 0.$$

Thus,

$$s = -v_s^2 \frac{\eta f_0}{4G(1+h)^2} k^2 \pm \frac{1}{2} \sqrt{\left(v_s^2 \frac{\eta f_0}{2G(1+h)^2} k^2 \right)^2 - 4v_s^2 \frac{h}{1+h} k^2}. \tag{3.21}$$

From (3.21), it is evident that the instability condition $\mathcal{R}[s] > 0$ is equivalent to having $h < 0$. Indeed, if we let $b = v_s^2 \frac{\eta f_0}{2G(1+h)^2} k^2$ and $c = v_s^2 \frac{h}{1+h} k^2$, then (3.21) is equivalent to

$$s = -\frac{b}{2} \pm \sqrt{\left(\frac{b}{2} \right)^2 - c}. \tag{3.22}$$

As $b > 0$, $\mathcal{R}[s] \leq 0$ whenever $c \geq 0$. In addition, if $c < 0$, which is equivalent to $h < 0$, then $\frac{b^2}{4} - c > \frac{b^2}{4}$, so that one solution of (3.22) is such that $s > 0$. This means that localization would occur only for strain softening materials. This is in agreement with what was observed for the elasto-plastic problem.

In addition, (3.21) shows that the growth coefficient s still has its maximum at $\lambda = 0$ as in the elasto-plastic case. Nonetheless, with contrast to what was observed in that case, the growth coefficient s is bounded here, as it can be seen in Figure 8.

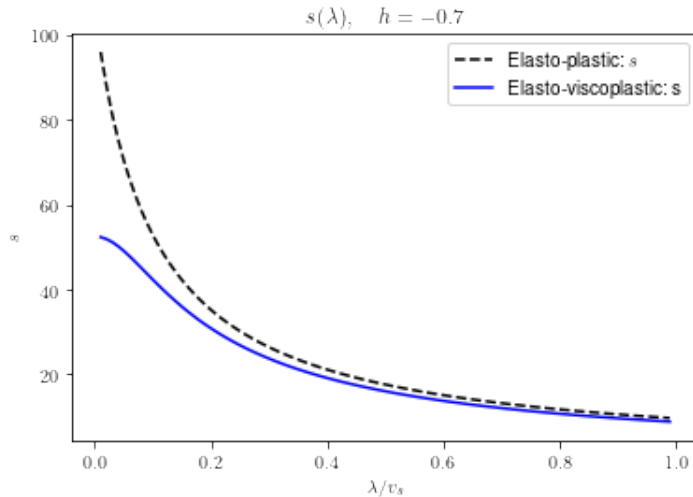


Figure 8: Perturbation growth coefficient s vs wavelength λ for a strain softening material with elasto-viscoplastic response under simple shearing. With contrast to the elasto-plastic case, the growth coefficient s is bounded as a result of viscous effects.

As a conclusion, viscous effects have the potential of alleviating the mesh-size dependency problem as they keep the growth coefficient bounded, but the approach does not regularize the strain localization problem as it is still independent of the wavelength λ , and predicted to occur for $\lambda = 0$.

We will see in the next section that the problem can be regularized using Cosserat continuum theory.

4 Cosserat continuum regularization

Cauchy continuum theory provides a macroscale description of materials. In that regard, a material is modeled as a continuous distribution of particles, each being represented by a point and can only translate when the material is under deformation. On the other hand, Cosserat continuum theory considers each particle of the material as a rigid body of non-negligible size, which can thus undergo both translations and rotations during deformations. This allows to take into account microscopic rotations and provides a more realistic framework for the study of localization problems [SG19].

By incorporating different scales, Cosserat theory naturally introduces internal length scales that allow the regularization of the strain localization problem. It is important to note that Cosserat continuum theory can be embedded in the general Micromorphic continua theory, which is part of the Multiscale modeling approach in Mathematics [SG19].

In what follows, we start by providing an overview of the Cosserat continuum theory and then use it to investigate the conditions for strain localization onset for the elasto-plastic problem studied earlier.

4.1 Mathematical description

For a Cosserat continuum, the Cauchy's momentum equation is replaced by the following equations [SG19][RSS18]:

$$\frac{\partial \tau_{ij}}{\partial x_j} + f_i = \rho \ddot{u}_i, \quad (4.1)$$

$$\frac{\partial m_{ij}}{\partial x_j} - \varepsilon_{ijk} \tau_{jk} + \psi_i = I \ddot{\omega}_i^c; \quad (4.2)$$

where:

- u_i is the displacement vector;
- $\omega_{ij}^c = -\varepsilon_{ijk} \omega_k^c$ is the micro-deformation tensor, called Cosserat rotation tensor;
- τ_{ij} is the Cosserat stress tensor, generally non-symmetric;
- m_{ij} is the Cosserat couple-stress tensor;
- f_i and ψ_i express body forces and moments, respectively;
- ρ is the material density, and I its micro-inertia; and
- ε_{ijk} is the Levi-Civita permutation symbol.

We saw that for a Cauchy continuum, deformations are described by the strain tensor ε_{ij} defined in (2.2). For a Cosserat continuum, deformations are described by a generalized strain tensor, γ_{ij} , and a curvature tensor κ_{ij} , as follows:

$$\gamma_{ij} = u_{i,j} + \varepsilon_{ijk} \omega_k^c, \quad (4.3)$$

$$\kappa_{ij} = \omega_{i,j}^c. \quad (4.4)$$

Hence, constitutive relations are of the form $\tau_{ij} = \tau_{ij}(\gamma_{ij}, \kappa_{ij})$ and $m_{ij} = m_{ij}(\gamma_{ij}, \kappa_{ij})$. It is usually convenient to split the strain tensor γ_{ij} into its symmetric part $\gamma_{(ij)}$ and antisymmetric part $\gamma_{[ij]}$, and so for the curvature tensor κ_{ij} . Doing so, (4.3) & (4.4) read [RSS18]:

$$\gamma_{(ij)} = \frac{1}{2} (u_{i,j} + u_{j,i}), \quad \Omega_{ij} = \frac{1}{2} (u_{i,j} - u_{j,i}), \quad (4.5)$$

$$\gamma_{[ij]} = \Omega_{ij} - \omega_{ij}^c, \quad \gamma_{ij} = \gamma_{(ij)} + \gamma_{[ij]}, \quad (4.6)$$

and similarly for κ_{ij} and τ_{ij} . The tensors $\gamma_{(ij)}$ and Ω_{ij} describe macroscopic strains and rotations (vorticity), while ω_{ij}^c describes rotations that occur at the micro-scale [RSS18]. Such decomposition into symmetric and antisymmetric parts can also be performed for the stress tensor τ_{ij} and the couple-stress tensor m_{ij} .

4.2 Regularization of an elasto-plastic localization problem

The strain localization problem that we investigate here comes from [SG19] and considers an elasto-plastic Cosserat medium with yield surface given by:

$$F = \tau_{(12)} - \tau_0, \quad (4.7)$$

where $\tau_{(12)}$ is the symmetric part of the stress tensor τ_{12} . The flow is assumed to be incompressible, and invariant in the x_1 and x_3 directions as in the Cauchy continuum case. In addition, the material is assumed to have an elasto-plastic behavior:

$$\dot{\gamma}_{ij} = \dot{\gamma}_{ij}^e + \dot{\gamma}_{ij}^p, \quad (4.8)$$

$$\dot{\kappa}_{ij} = \dot{\kappa}_{ij}^e + \dot{\kappa}_{ij}^p; \quad (4.9)$$

where the elastic response is determined by the following constitutive laws:

$$\tau_{ij} = K\gamma_{kk}^e + 2G \left(\gamma_{(ij)}^e - \frac{1}{3}\gamma_{kk}^e\delta_{ij} \right) + 2\eta_1 G\gamma_{[ij]}^e, \quad (4.10)$$

$$m_{ij} = 4GR^2 (\kappa_{ij}^e + \eta_2\kappa_{kk}^2\delta_{ij}) + 4\eta_3 GR^2\kappa_{[ij]}^e; \quad (4.11)$$

where the η_i , $i = 1, 2, 3$, are positive material parameters, and K and G are, respectively, the bulk and shear moduli, as before. Here, the particles of the Cosserat medium are identified as spherical grains of radius R and negligible mass. This implies that the micro-inertia is $I = \frac{R^2}{2}$ in 2D, or $I = \frac{2}{5}R^2$ in 3D [RSS18]. As the flow is incompressible, and invariant in the x_1 and x_3 directions, the balance equations (4.1)-(4.2) reduce to:

$$\frac{\partial\tau_{12}}{\partial x_2} + f_1 = \rho\ddot{u}_1; \quad (4.12)$$

$$\frac{\partial m_{32}}{\partial x_2} + \tau_{21} - \tau_{12} + \psi_3 = I\ddot{\omega}_3^c. \quad (4.13)$$

We now assume that at steady we have a Cauchy continuum under homogeneous shear, so that $\tau_{(12)} = \tau_{(12)}^* = \tau_0$, $\tau_{[12]} = \tau_{[12]}^* = 0$, $m_{32} = m_{32}^* = 0$, and $u_i = u_i^*$, $\omega_i^c = \omega_i^{c*}$. We are interested in the conditions under which this homogeneous state will be unstable, leading to strain localization. Proceeding the same way as we did for the Cauchy continuum, we perturb kinematic fields around the steady state:

$$u_i = u_i^* + \tilde{u}_i \quad \text{and} \quad \omega_i^c = \omega_i^{c*} + \tilde{\omega}^c. \quad (4.14)$$

Taking this in (4.12) & (4.13), we obtain:

$$\frac{\partial\tilde{\tau}_{12}}{\partial x_2} = \rho\ddot{\tilde{u}}_1; \quad (4.15)$$

$$\frac{\partial\tilde{m}_{32}}{\partial x_2} + \tilde{\tau}_{21} - \tilde{\tau}_{12} = I\ddot{\tilde{\omega}}_3^c. \quad (4.16)$$

As in the previous section, we have now to find new constitutive relations describing the perturbed system. From (4.10), we have:

$$\tilde{\tau}_{12} = 2G\tilde{\gamma}_{(12)}^e + 2G\eta_1\tilde{\gamma}_{[12]}^e,$$

from which we have:

$$\tilde{\tau}_{(12)} = 2G\tilde{\gamma}_{(12)}^e, \quad \text{and} \quad (4.17)$$

$$\tilde{\tau}_{[12]} = 2G\eta_1\tilde{\gamma}_{[12]}^e = 2G\eta_1\tilde{\gamma}_{[12]}; \quad (4.18)$$

where we have taken $\tilde{\gamma}_{[12]}^p = 0$ for simplicity. This means that at the macroscopic scale, plastic deformations of the Cosserat medium are taken to be identical to plastic strains for a Cauchy continuum. Proceeding the exact same way as in the derivation of (3.4), (4.17) yields:

$$\tilde{\tau}_{(12)} = 2G\frac{h}{1+h}\tilde{\gamma}_{(12)}. \quad (4.19)$$

Similarly, (4.11) yields:

$$\tilde{m}_{32} = 4GR^2\tilde{\kappa}_{32}, \quad (4.20)$$

where we have again taken $\eta_3 = 1$ for simplicity.

From here, the idea is to assume that the perturbations \tilde{u}_1 and $\tilde{\omega}_3^c$ are plane waves, i.e.

$$\tilde{u}_1 = U_1 e^{st+ikx_2}, \quad (4.21)$$

$$\tilde{\omega}_3^c = \Omega_3 e^{st+ikx_2}; \quad (4.22)$$

and use the governing equations (4.15) & (4.16), and the constitutive relations (4.18)-(4.20) to derive an equation relating the growth coefficient s to material parameters.

From (4.15), we have:

$$\begin{aligned}
\rho \ddot{u}_1 &= \frac{\partial \tilde{\tau}_{12}}{\partial x_2} \\
&= \frac{\partial \tilde{\tau}_{(12)}}{\partial x_2} + \frac{\partial \tilde{\tau}_{[12]}}{\partial x_2} \\
&= 2G \frac{h}{1+h} \frac{\partial \tilde{\gamma}_{(12)}}{\partial x_2} + 2G\eta_1 \frac{\partial \tilde{\gamma}_{[12]}}{\partial x_2} \quad \text{by (4.18) \& 4.19} \\
&= G \frac{h}{1+h} \frac{\partial^2 \tilde{u}_1}{\partial x_2^2} + G\eta_1 \frac{\partial^2 \tilde{u}_1}{\partial x_2^2} + 2G\eta_1 \frac{\partial \tilde{\omega}_3^c}{\partial x_2} \quad \text{by (4.4) - (4.6)}
\end{aligned}$$

Taking (4.21) and (4.22) into this last equation yields:

$$\left[Gk^2 \left(\eta_1 + \frac{h}{1+h} \right) + \rho s^2 \right] U_1 - i 2k\eta_1 G \Omega_3 = 0. \quad (4.23)$$

Considering the other governing equation, and using $I = \frac{R^2}{2}$, we obtain:

$$\begin{aligned}
\frac{\partial \tilde{m}_{32}}{\partial x_2} + \tilde{\tau}_{21} - \tilde{\tau}_{12} &= \frac{R^2}{2} \ddot{\omega}_3^c, \\
\frac{\partial \tilde{m}_{32}}{\partial x_2} - 2\tilde{\tau}_{[12]} &= \frac{R^2}{2} \ddot{\omega}_3^c \quad \text{since } \tilde{\tau}_{(21)} = \tilde{\tau}_{(12)} \quad \text{and } \tilde{\tau}_{[21]} = -\tilde{\tau}_{[12]}, \\
4GR^2 \frac{\partial \tilde{\kappa}_{32}}{\partial x_2} - 4G\eta_1 \tilde{\gamma}_{[12]} &= \frac{R^2}{2} \ddot{\omega}_3^c \quad \text{by (4.18) \& (4.20),} \\
4GR^2 \frac{\partial^2 \tilde{\omega}_3^c}{\partial x_2^2} - 4G\eta_1 \tilde{\omega}_3^c - 2G\eta_1 \frac{\partial u_1}{\partial x_2} &= \frac{R^2}{2} \ddot{\omega}_3^c \quad \text{by (4.4) - (4.6).}
\end{aligned}$$

Taking (4.21) & (4.22) into this last equation, we obtain:

$$i4Gk\eta_1 U_1 + [8G(\eta_1 + k^2 R^2) + R^2 s^2] \Omega_3 = 0. \quad (4.24)$$

Equations (4.23) and (4.24) form a linear system, which, in matrix notation, gives:

$$\begin{bmatrix} Gk^2 \left(\eta_1 + \frac{h}{1+h} \right) + \rho s^2 & -i 2k\eta_1 G \\ i4Gk\eta_1 & 8G(\eta_1 + k^2 R^2) + R^2 s^2 \end{bmatrix} \begin{bmatrix} U_1 \\ \Omega_3 \end{bmatrix} = 0. \quad (4.25)$$

Since $U_1 \neq 0$ and $\Omega_3 \neq 0$, (4.25) yields:

$$\det \begin{bmatrix} Gk^2 \left(\eta_1 + \frac{h}{1+h} \right) + \rho s^2 & -i 2k\eta_1 G \\ i4Gk\eta_1 & 8G(\eta_1 + k^2 R^2) + R^2 s^2 \end{bmatrix} = 0;$$

from which we obtain:

$$R^2 \rho s^4 + [GR^2 k^2 (H + \eta_1 + 8\rho) + 8G\eta_1 \rho] s^2 + 8G^2 k^2 R^2 \left[k^2 (H + \eta_1) + \frac{H\eta_1}{R^2} \right] = 0; \quad (4.26)$$

or

$$\xi^2 + b\xi + c = 0, \quad (4.27)$$

where

$$\xi = s^2, \quad H = \frac{h}{1+h}, \quad (4.28)$$

$$b = v_s^2 k^2 (H + \eta_1) + 8G \left(k^2 + \frac{\eta_1}{R^2} \right) \quad (4.29)$$

$$c = 8G v_s^2 k^2 \left[\left(k^2 + \frac{\eta_1}{R^2} \right) H + \eta_1 k^2 \right] \quad (4.30)$$

Letting $\Delta = b^2 - 4c$, the growth coefficient s is given by

$$s = \pm \sqrt{-\frac{b}{2} \pm \sqrt{\frac{b^2}{4} - 2c}}, \quad (4.31)$$

with the following cases.

1. $\Delta < 0 \Rightarrow \mathcal{S}[\xi_1] \neq 0$ and $\mathcal{S}[\xi_2] \neq 0$. Since the square roots of a complex number are π radians apart on a circle, and $b \neq 0$, two solutions of (4.26) are such that $\mathcal{R}[s] > 0$. Hence, strain localization is expected when $\Delta > 0$.
2. $\Delta = 0 \Rightarrow \xi = -\frac{b}{2}$. If $b \geq 0$, then $\mathcal{R}[s] = 0$. Otherwise, one solution of (4.26) is such that $\mathcal{R}[s] > 0$, and the homogeneous deformation state is unstable.
3. $\Delta > 0 \Rightarrow \mathcal{S}[\xi_1] = \mathcal{S}[\xi_2] = 0$. In this case, we have the following scenarios.
 - If $b > 0$ and $c > 0$, then $\xi_1 < 0$ and $\xi_2 < 0$. Hence, $\mathcal{R}[s] < 0$, and the homogeneous state is stable.
 - If $b < 0$ and $c > 0$, then $\xi_1 > 0$ and $\xi_2 > 0$. Therefore, (4.26) has two solutions such that $\mathcal{R}[s] > 0$, implying that the homogeneous deformation state is unstable.
 - If $c < 0$, then for all values of b , $\xi_1 > 0$ and $\xi < 0$. Hence, (4.26) has one solution such that $\mathcal{R}[s] > 0$. Notice that whenever $c < 0$, $\Delta > 0$. This means that the condition $c < 0$ is sufficient for strain localization. In addition, it is evident from (4.30) that to have $c < 0$, we have to have:
 - $H < 0$, which is equivalent to $h < 0$, and
 - $(k^2 + \frac{\eta_1}{R^2}) H + \eta_1 k^2 < 0$, or equivalently

$$\begin{aligned} \lambda > \lambda_c &= 2\pi R \sqrt{-\left(\frac{1}{H} + \frac{1}{\eta_1}\right)} \\ &= 2\pi R \sqrt{-\frac{1+h}{h} - \frac{1}{\eta_1}} \end{aligned} \quad (4.32)$$

This shows that, for a Cosserat continuum, the strain softening condition is not sufficient for strain localization. The wavelength of perturbation has, in addition, to be larger than the critical value given in (4.32) for localization to occur. This is in contrast with the observation made for Cauchy continua, and showcases the effectiveness of the Cosserat continuum theory in the regularization of the strain localization problem. In addition (4.32) shows that λ_c is proportional to the Cosserat internal length, R . In Figure 9, we plot the perturbation growth coefficient s vs the wavelength λ in the case $c < 0$. Notice that s stays finite for a Cosserat material, and the strain localization problem is regularized as the s reaches its maximum for a value of $\lambda > \lambda_c > 0$. It is important to note that (4.32) comes with the extra condition that $\eta_1 + \frac{h}{1+h} < 0$.

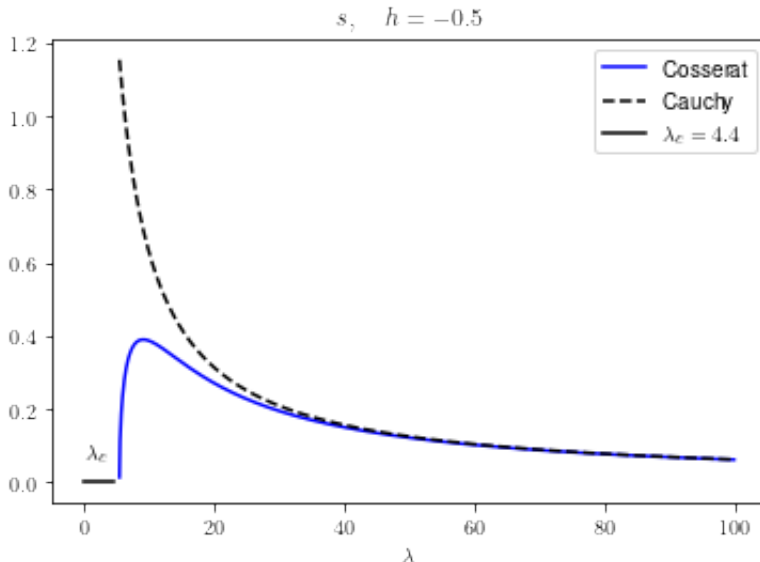


Figure 9: Perturbation growth coefficient s vs wavelength λ for a Cosserat strain softening material with linear elasto-plastic response under simple shearing. With contrast to the Cauchy material, the wavelength of the perturbation has to be larger than a critical value λ_c for strain localization to occur. This showcases the effectiveness of the Cosserat continuum regularization.

It is worth noting that though Stefanou et al. [SG19] stated the same expression for the critical wavelength λ_c , (4.32 cannot be derived from their expression for the perturbation growth coefficient s . In addition, we would like to emphasize that we failed to derive a critical wavelength using the simplifying assumption $I = 0$ used in [SG19]. This might be due to the fact that I is proportional to the internal length R , which plays a key role in Cosserat regularization. Moreover, we think that assuming $I = 0$ can be very confusing as it is the same as assuming $R = 0$. An alternative assumption to $I = 0$, which Stefanou et al [SG19] probably meant, would be $\tilde{\omega}_3^c = 0$. Nonetheless, we think that neither this assumption, nor $I = 0$, should be considered when studying the strain localization problem.

5 Conclusion

In this research, we explored the plastic strain localization phenomenon which is ubiquitous in materials, especially geomaterials. We started by reviewing the underlying concepts from continuum mechanics and then we presented how perturbation theory can be used to derive conditions for localization in a rather hands-on approach. We showed that strain localization is expected for strain softening Cauchy materials with an elastoplastic response. In addition, we observed that the growth coefficient of the perturbation was predicted to become unbounded at vanishing perturbation wavelengths, resulting in a temporal singularity. As a consequence, the width of the localization zone was unrealistically predicted to be zero (spatial singularity) [SG19]. To avoid these issues, some regularization techniques were introduced. Specifically, we explored viscous regularization and showed that though it fixed the temporal singularity problem by keeping the growth coefficient bounded at vanishing wavelengths, it still predicted the occurrence of strain localization on a mathematical plane. We went on exploring the Cosserat continuum theory and how can be used in regularizing the strain localization problem. This approach proved to be very effective in remedying both the temporal and spatial singularities. The effectiveness of the Cosserat continuum approach was attributed to the inter-

nal wavelength it embodies. Indeed, by taking into account the both the macroscopic and microscopic scales of materials, the Cosserat continuum theory introduces internal length scales that the classical Cauchy continuum failed to take into account, and the predictions showed that these internal length scales play a major role in the regularization of the strain localization problem.

Acknowledgements

This research was carried as part of the Mfano Africa-Oxford Virtual Mentorship Programme. We would like to express our gratitude to Professor Richard F. Katz for his willingness to supervise this research and for the special attention that he has given us during all the stages of this project. We would also like to thank the Mathematical Institute at the University of Oxford, Mfano Africa and all the people involved for the opportunity given us to be part of the life-changing Mfano Africa-Oxford Virtual Mentorship Programme.

References

- [How17] Peter Howell. Elasticity and plasticity (lecture notes). 2017.
- [Kel] PA Kelly. Mechanics lecture notes: An introduction to solid mechanics. <http://homepages.engineering.auckland.ac.nz/~pkel015/SolidMechanicsBooks/index.html>.
- [RSS18] Hadrien Rattiez, Ioannis Stefanou, and Jean Sulem. The importance of thermo-hydro-mechanical couplings and microstructure to strain localization in 3d continua with application to seismic faults. part i: Theory and linear stability analysis. *Journal of the Mechanics and Physics of Solids*, 115:54–76, 2018.
- [SG19] Ioannis Stefanou and Eleni Gerolymatou. Strain localization in geomaterials and regularization: rate-dependency, higher order continuum theories and multi-physics. https://coquake.eu/wp-content/uploads/2019/10/ALERT_2019.pdf, 2019.
- [Wik] Wikipedia. Necking (engineering). [https://en.wikipedia.org/wiki/Necking_\(engineering\)](https://en.wikipedia.org/wiki/Necking_(engineering)) (accessed: 06-09-2021).